Proceedings of the Sixth International Conference on
Railway Technology: Research, Development and Maintenance
Edited by: J. Pombo
Civil-Comp Conferences, Volume 7, Paper 15.7
Civil-Comp Press, Edinburgh, United Kingdom, 2024
ISSN: 2753-3239, doi: 10.4203/ccc.7.15.7

Drive-By Early Damage Detection in Railway Bridges using Wavelets and Autoencoders

C. Braganca[1], E. D. De Souza[1,2], D. Ribeiro[3] and T. Bittencourt[1]

[1]Department of Structural and Geotechnical Engineering, University of São Paulo, Brazil
[2]School of Engineering, Federal Technological University of Paraná, Brazil
[3]CONSTRUCT-LESE, School of Engineering, Polytechnic of Porto, Portugal

Abstract

This paper presents an innovative AI-driven drive-by methodology for unsupervised damage detection on a Warren truss bridge. The methodology employs acceleration data collected from eight sensors mounted on a LAAGRSS-type freight wagon. Wavelet scattering coefficients derived from these acceleration signals serve as input features for the model. Autoencoders, trained on baseline condition data, are utilized to reconstruct these coefficients, with the absolute reconstruction error acting as a damage-sensitive feature. Environmental and operational variations are mitigated through normalization, excluding high-variability components. A three-level data fusion approach, based on the Mahalanobis distance, generates a highly sensitive damage indicator. This indicator accurately detects all simulated damage scenarios, including those in their early stages, without misclassification. The study demonstrates the efficacy of the proposed methodology also for distinguishing between different damage types. Future work will focus on experimental validation and enhancement of the methodology for assessing damage severity.

Keywords: drive-by, damage identification, vehicle-structure interaction, wavelet scattering transform, autoencoders, data fusion.

1 Introduction

Bridge health monitoring is crucial for maintaining the safety and functionality of railway infrastructure. Traditional methods of damage detection often require manual inspections, mainly based on visual checks, which can be time-consuming, costly and not efficient in early real time damage detection [1]. Within this context researchers have sought for more efficient and cheaper techniques. The concept of using vehicles as moving sensors (Figure 1), known as drive-by monitoring, comes as an economic alternative for monitoring large-scale infrastructures like railways, in which the instrumentation of the whole infrastructure is not feasible [1,2].

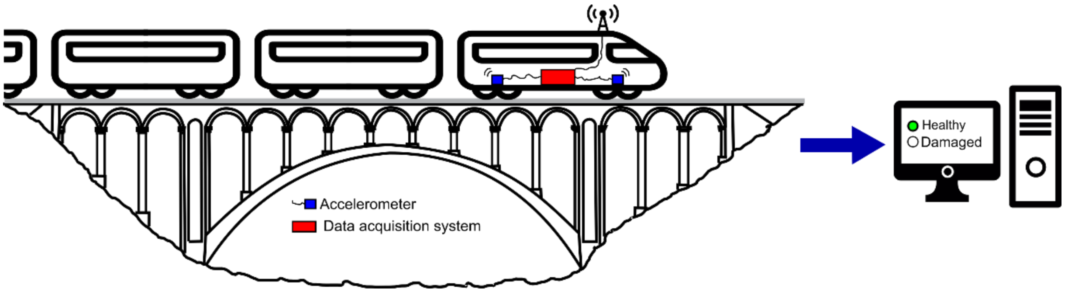

Figure 1: Indirect bridge monitoring concept.

The drive-by concept was first introduced by Yang et al. [3], who demonstrated the feasibility of extracting bridge natural frequencies from acceleration records collected inside road vehicles. Since this pioneering work, numerous researchers have focused on developing new methodologies to extract not only natural frequencies but also other modal properties such as mode shapes and damping ratios, along with techniques for damage detection. For a comprehensive review of drive-by methodologies applied to railway infrastructures, refer to [4,5].

More recently, advancements in AI and data processing have been offering new possibilities for automated and unsupervised drive-by damage detection systems. In this context, the present work introduces an innovative AI-driven methodology for unsupervised damage detection on a Warren truss bridge. The proposed approach leverages acceleration data from a virtual monitoring system, consisting of eight sensors mounted on a LAAGRSS-type freight wagon. By computing wavelet scattering coefficients (WSC) from the acceleration signals, the methodology extracts features that are sensitive to bridge damage conditions.

Initially, autoencoders are trained using a baseline scenario to reconstruct the WSCs, and the absolute reconstruction error (ARE) is then used as a damage-sensitive feature. To eliminate environmental and operational influences, normalization is performed using Principal Component Analysis (PCA). The methodology further integrates a three-level data fusion based on the Mahalanobis distance, combining frequency, sensor, and time dimensions into a single damage indicator. This robust indicator can detect damage at various stages without any misclassification. The proposed approach's efficacy is demonstrated through numerical simulations, highlighting its potential for early-stage damage detection.

2 Damage identification methodology

A flowchart of the proposed AI-driven bridge damage identification methodology is presented in Figure 2.

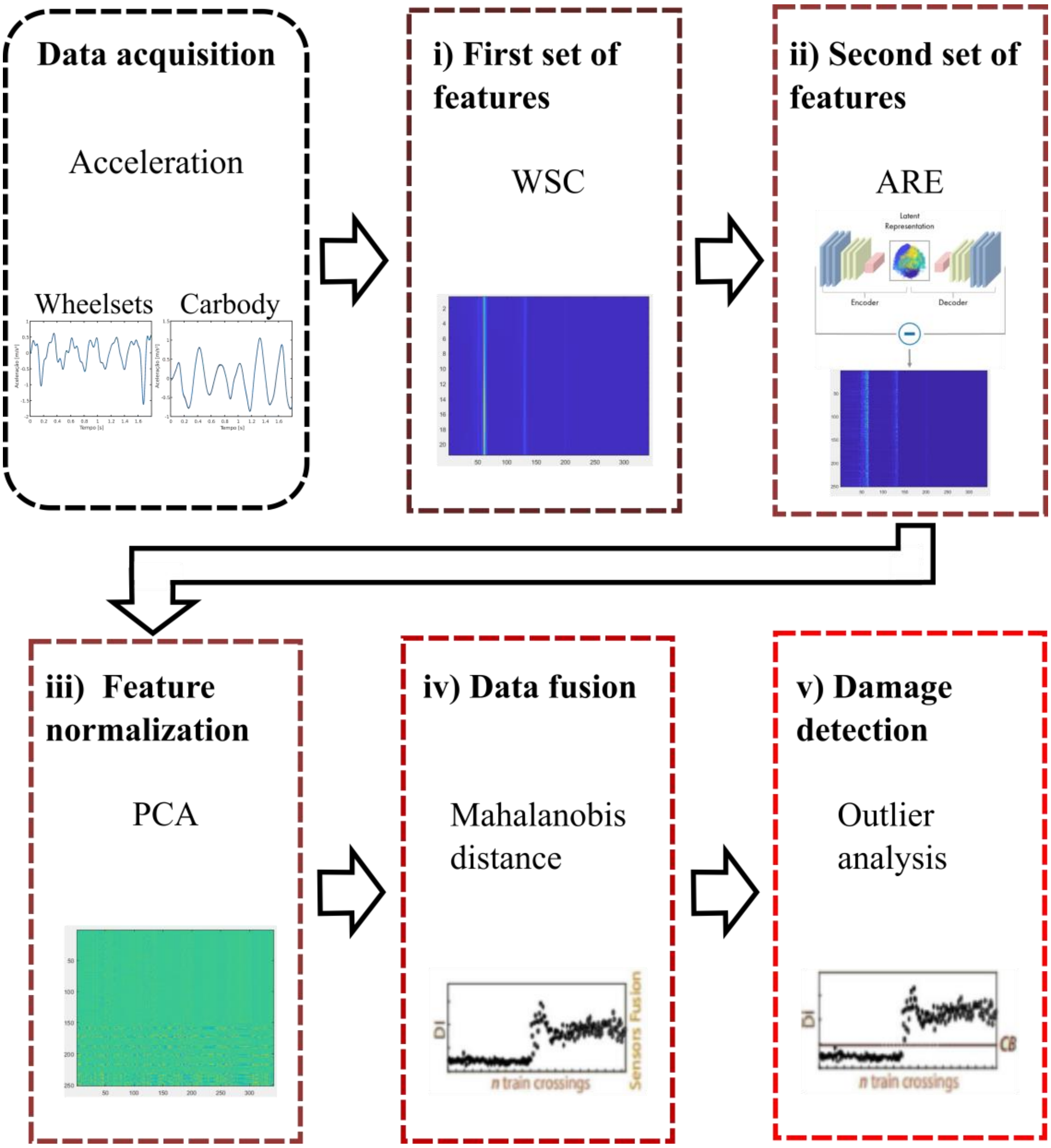

Figure 2: Flowchart of the proposed methodology.

The proposed methodology utilizes a virtual monitoring system composed of 8 acceleration sensors positioned on the first wagon of a train. The sensors are placed on both sides of the two axles and at four points directly above the wagon's suspensions. The accelerations recorded at these points serve as inputs for the methodology. The proposed methodology involves a 5-step process implemented in MATLAB® [6], detailed as follows:

I. A preliminary set of features is extracted based on the wavelet scattering coefficients (WSC) of the acceleration signals computed for each sensor. This step is crucial for deriving time series properties that are more sensitive to the bridge damage condition.

II. Eight autoencoders (one for each sensor) are then trained to reconstruct the WSCs from a baseline scenario, consisting of data acquired when the bridge is undamaged. A new feature is extracted based on the absolute reconstruction error (ARE) of the autoencoders computed individually for every scattering coefficient (time and frequency dimensions).

III. Normalization of this new features is performed using the Principal Component Analysis (PCA) to remove the effects of operational and environmental variations. In this process the components associated with a larger variability are removed, since these are typically related to environmental or operational factors.

IV. A three-level data fusion based on the Mahalanobis distance is performed. First, the WSCs associated with different frequencies are fused into a single indicator. Next, a sensor fusion is conducted. Finally, a fusion in the time dimension is performed, combining the time components into a single damage indicator.

V. Lastly, automatic damage detection is carried out using outlier analysis.

3 Numerical simulations

In this section a brief overview of the numerical methodology used for validating the proposed methodology is presented. Firstly, the numerical models of the three railway subsystems (vehicle, track, and bridge) are presented. Later one details regarding the numerical vehicle-structure interaction simulation as well as the scenarios studied are presented.

3.1 Freight wagon numerical model

The wagon used in the simulations is a Laargss-type freight wagon (Figure 3a). This specialized wagon is designed for transporting containers and travels along the Beira Alta line of the Portuguese railway network, where it serves to transport paper rolls. Measuring 14.8 m in length, this wagon is supported by two axles spaced 10 m apart. The connection between the axles and the body is facilitated by four sets of progressive stiffness parabolic springs, secured by UIC double links. All the suspension system is standardized following the recommendations from [7]. With a tare weight of 27.1 t, the wagon has the capacity to carry loads of up to 24.9 t, totalizing 52 t. A multi-body type modeling strategy (Figure 3b) was chosen due to is low computational cost and good representation of the global wagon behavior [8]. The model features rigid bars to represent the wagon's structure, with the suspensions being modeled by spring-damper elements, these being the only flexible components in the model.

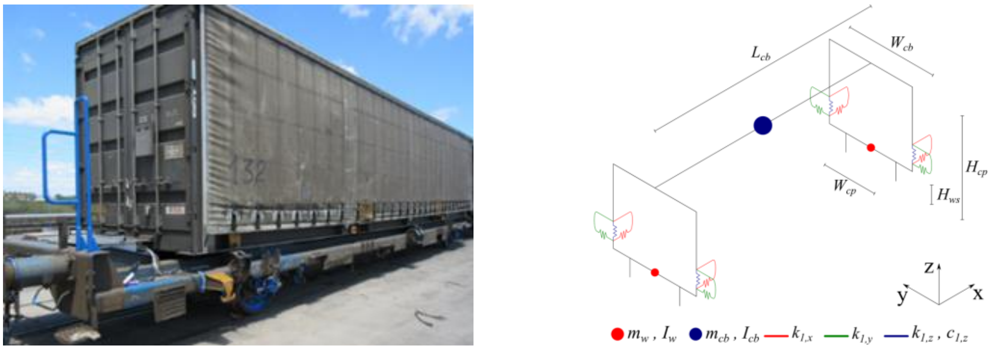

(a) (b)

Figure 3: Laargss-type Freight wagon: (a) wagon view and (b) numerical model.

The properties adopted for the numerical model are depicted in Table 1, based on the ones calibrated by [8] using experimental modal information.

Table 1: Properties of the wagon numerical model [8]

Parameter	Symbol (Unit)	Calibrated Value
Car Body		
Mass	m_{cb} (ton)	45.72
Moment of inertia about longitudinal axis	$I_{cb,x}$ (t.m^2)	49
Moment of inertia about transverse axis	$I_{cb,y}$ (t.m^2)	562.8
Moment of inertia about vertical axis	$I_{cb,z}$ (t.m^2)	665
Length	L_{cb} (m)	10.000
Width	W_{cb} (m)	2.170
Height above ground	H_{cb} (m)	2.297
Wheelsets		
Mass	m_w (kg)	1247
Moment of inertia about longitudinal axis	$I_{w,x}$ (kg.m^2)	312
Moment of inertia about vertical axis	$I_{w,z}$ (kg.m^2)	312
Track Gauge	W_{cp} (m)	1.668
Height above ground (wheelset)	H_{ws} (m)	0.450
Suspensions		
Longitudinal stiffness	$k_{1,x}$ (kN/m)	44981
Lateral stiffness	$k_{1,y}$ (kN/m)	30948
Vertical stiffness	$k_{1,z}$ (kN/m)	2252.7
Vertical damping	$c_{1,z}$ (kN.s/m)	35.73

3.2 Track numerical model

The numerical model of the track was developed using ANSYS® [9], based on the model described by Neto et al. [10]. This model consists of 3 layers representing the ballast, sleepers, and rails, which are interconnected through appropriate interfaces. The foundation level of the model is fully fixed, while the longitudinal stiffness of the track is provided by the springs' longitudinal stiffness in the different interfaces.

Finite beam elements (BEAM4) are used to model the rails and sleepers, spring-damper elements (COMBIN14) are used for the ballast, clamp, and foundation interfaces, and point masses (MASS21) are added at the ends of the sleepers, as illustrated in Figure 4. The mechanical properties of the track components were adopted from the literature and are detailed in Table 2 as well as the symbols for these properties.

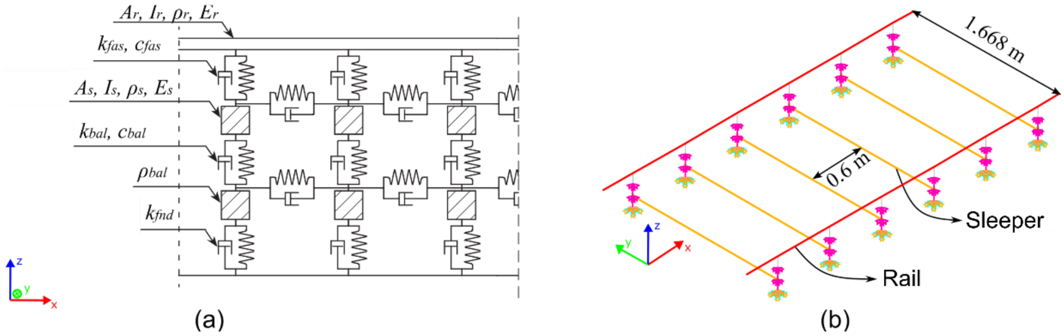

Figure 4. Three-layer numerical model of the track: (a) Schematic representation and (b) three-dimensional model

Table 2: Properties of the track numerical model.

Component	Parameter	Description	Value	Reference
	A_r	Inertia (cm^4)	76,7	
	I_r	Density (kg/m^3)	3038	
Rail (UIC60)	ρ_r	Elastic Modulus (GPa)	7850	[11]
	E_r	Longitudinal/Transverse Stiffness (MN/m)	210	
	$k_{fas,l/t}$	Longitudinal/Transverse Damping (kN.s/m)	20	[12]
	$c_{fas,l/t}$	Vertical Stiffness (MN/m)	50	
Clamps/Pads	$k_{fas,v}$	Vertical Damping (kN.s/m)	500	
	$c_{fas,v}$	Rotational Stiffness (kN.m/rad)	200	[13]
	$k_{fas,r}$	Area (cm^2)	45	[14]
	A_s	Inertia (cm^4)	402,5	
	I_s	Density (kg/m^3)	17620	
Sleepers	ρ_s	Elastic Modulus (GPa)	2500	[15]
	E_s	Longitudinal Stiffness (MN/m/m)	40,9	
	$k_{bal,l}$	Transverse Stiffness (MN/m/m)	30	[16]
	$k_{bal,t}$	Vertical Stiffness (MN/m/m)	7,5	
Ballast	$k_{bal,v}$	Damping in All Directions (kN.s/m/m)	100	[14]
	c_{bal}	Density (kg/m^3)	50	
	ρ_{bal}	Vertical Stiffness (MN/m)	1995,9	[15]
Foundation	$k_{fnd,v}$	Inertia (cm^4)	20	[17]

To better approximate real-world conditions in the track modeling, the simulations incorporate artificially generated railway irregularity profiles based on power spectral density functions, covering wavelengths from 1 m to 75 m with a resolution of 0.01 m. These irregularities were introduced into the simulations using the VSI numerical interaction tool, as detailed in Section 3.4.

3.3 Bridge numerical model

The numerical model of the bridge was developed and calibrated based on data provided by [18]. The bridge studied is an open Warren-type metal truss with a span of 21.42 m. For the design of its numerical model, ANSYS® [9] software and BEAM188 elements were used. The track was directly attached to the bridge structure with fixed connections to the crossbeams, eliminating the need for a ballast interface, as detailed in the construction specifications of [18]. A visual representation of the bridge model, indicating the elements to be evaluated in damage detection analyses, is shown in Figure 5. Damage is introduced in two distinct elements: one in a secondary component, a diagonal of the truss, and another in a more heavily stressed component, the lower chord of the truss bridge.

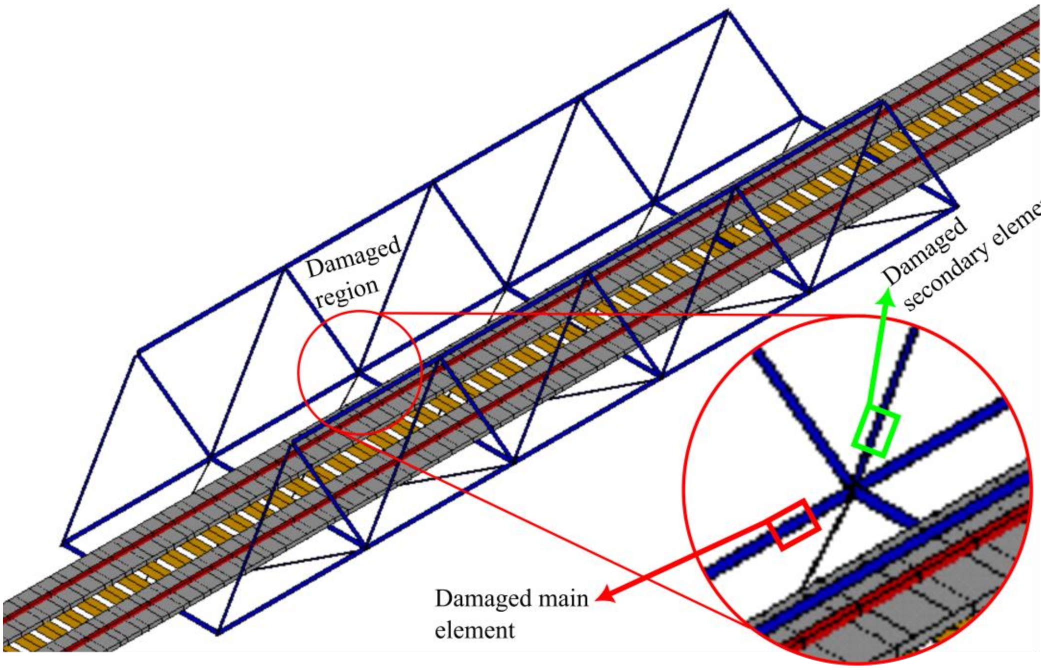

Figure 5. Bridge numerical model with the damaged elements

3.4 Vehicle structure interaction

To conduct the simulations, the numerical tool "VSI - Vehicle Structure Interaction Analysis" was employed. Initially proposed by [13] and subsequently enhanced by [14] to incorporate lateral interaction in the wheel-rail contact model, this tool utilizes a 3D wheel-rail contact element that connects the different subsystems. This element manages the contact interface by computing the wheel-rail contact forces in the normal and tangential directions. During each time interval, the position of the contact point is determined, and the normal contact force is calculated using the nonlinear theory of Hertz [15]. The forces in the directions tangential to the contact plane are calculated based on Kalker's rolling contact theory [22], which is a function of the "creepage" velocities between the wheel and the rail and the shape of the contact ellipse. These forces are computed based on the USETAB book of tables [23], considering track irregularities. The tool directly integrates the structural matrices of the numerical models in ANSYS® [9] for vehicle and structure, using MATLAB® [6]. This integration leverages the complexity of commercial FEM software while benefiting from the efficiency of MATLAB® [6] programming. Figure 6 provides an overview of the VSI numerical tool. With such a tool, it is possible to accurately simulate dynamic responses (accelerations, velocities, and displacements) at any point in the structure.

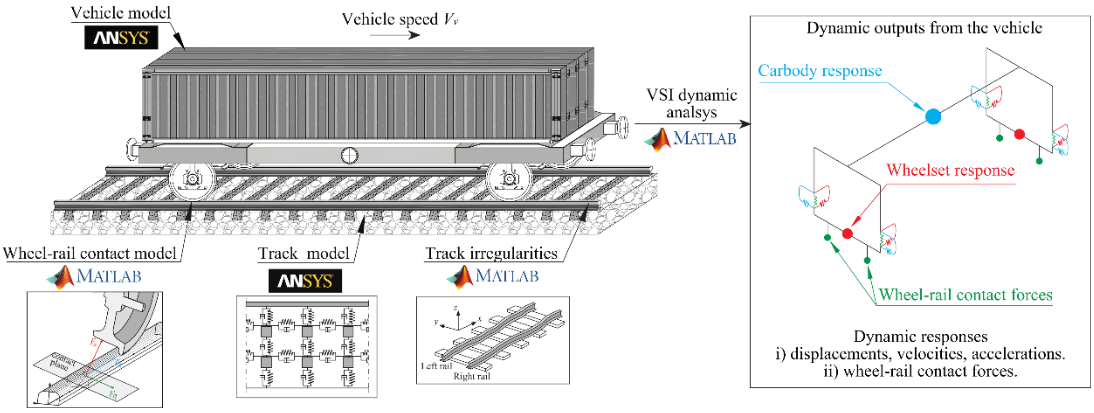

Figure 6. Framework of the VSI numerical tool

All simulations in this study were conducted with a sampling frequency of 1,000 Hz to accurately capture the problem's dynamics. This frequency was chosen based on a sensitivity analysis that assessed its impact on the results.

3.5 *Simulation scenarios*

The proposed methodology was validated through a series of numerical simulations, encompassing both a baseline scenario (without damage) and various damage scenarios. To simulate common operational interferences in railway operations, these scenarios incorporated a range of operational and environmental factors, including different speeds, irregularity profiles, mass variations, variations in elastic modulus with temperature, measurement noise, and wagon positioning inaccuracies. The specific conditions applied to the baseline and damage scenarios are detailed in Tables 3 and 4, respectively.

Table 3: Baseline simulation scenarios

Condition	**Five LAAGRSS type freight wagons**
Speeds (km/h)	40/45/50/55/60
Irregularity profiles	2
Wagon mass variation (%)	90/95/100/105/110
Variation in elastic modulus with temperature (‰)	975/1000/1025
Positioning accuracy (m)	±1
Measurement noise (%)	5

Table 4: Damage simulation scenarios.

Condition	Five LAAGRSS type freight wagons
Speeds (km/h)	45/50/55
Positioning accuracy (m)	±1
Measurement noise (%)	5
Damage scenarios (%)	1/2/5/10/20/30/50
Individually damaged elements	2

3.6 Dynamic responses

As an example, Figure 7 illustrates the acceleration responses of the first wagon as it crosses the bridge at a speed of 50 km/h, considering various damage levels in the diagonal of the warren truss bridge (secondary element). Section (a) of the figure shows the vertical accelerations on the left side of the front wheelset, while section (b) displays the vertical accelerations on the left front side of the wagon body, directly above the suspension. All timeseries data were filtered using a Chebyshev II low-pass digital filter with a cutoff frequency of 500 Hz. The analysis of these responses underscores the inherent complexity of damage identification, demonstrated by the subtle variations in the acceleration signals induced by the damage.

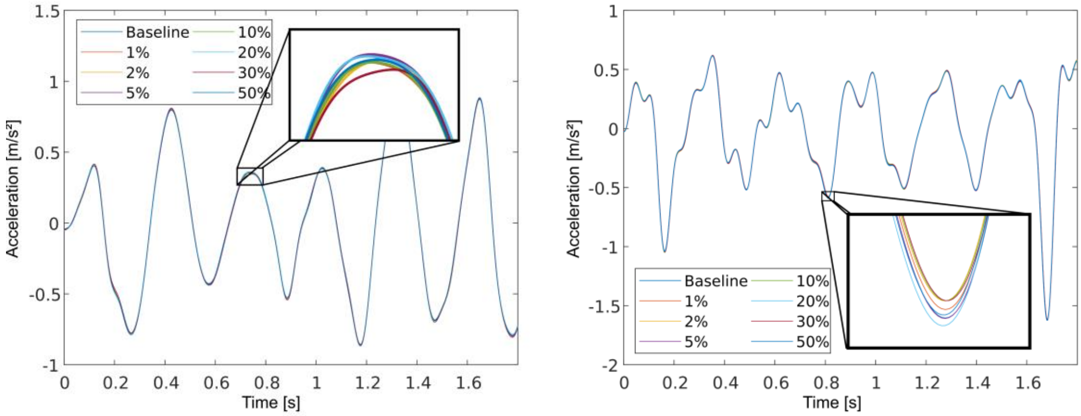

(a) (b)

Figure 7. Acceleration response in the wagon considering different damage scenarios: (a) Car body and (b) front wheelset of the 1st wagon

4 Results and discussion

Figure 8 presents the results of applying the methodology outlined in Section 2 to various simulation data sets. Red diamonds represent different damage scenarios, arranged in increasing order of severity. Train passes numbered above 146 correspond to scenarios with progressively more severe simulated damage. The figure demonstrates the proposed methodology's effectiveness in detecting damage, even in its earliest stages. The logarithmic scale on the vertical axis underscores the exceptionally high sensitivity of the methodology, since the damage scenarios can present DIs more than 3 orders of magnitude above the baseline cases. Additionally, a clear distinction can be observed between the damage scenarios associated with the truss diagonal (secondary damage) and the lower chord (main damage). This demonstrates that the proposed methodology is sensitive to damage severity. However, further refinement is necessary for accurately classifying the severity of damage at the same location.

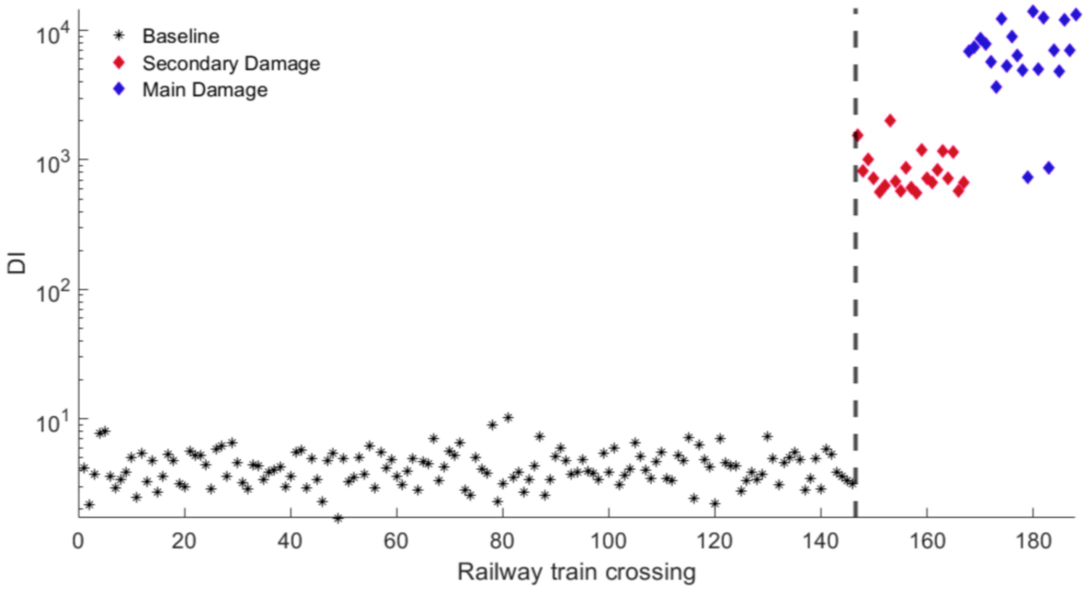

Figure 8. Damage detection on the warren truss bridge

5 Conclusions

This paper presents an innovative AI-driven methodology for unsupervised damage detection on a Warren truss bridge. Initially, acceleration data from 8 points on a LAAGRSS-type freight wagon were used to calculate wavelet scattering coefficients. These coefficients, associated with a baseline condition, were employed to train autoencoders for reconstruction, with the absolute reconstruction error serving as a damage-sensitive feature. To account for environmental and operational influences, high-variability components were excluded through normalization. A three-level data fusion based on the Mahalanobis distance was then applied to create a highly sensitive damage indicator. This indicator enabled accurate detection of all damage scenarios, including those in very early stages, without any misclassification, demonstrating the effectiveness of the proposed methodology. In future work, the authors plan to experimentally validate the methodology and enhance its capabilities for assessing damage severity.

Acknowledgements

The authors would like to thank CNPq (National Council for Scientific and Technological Development), CAPES (Coordination for the Improvement of Higher Education Personnel), FAPESP (São Paulo Research Foundation) for the financial support provided through grant #2022/13045-1, VALE Cátedra Under Rail, and Base Funding - UIDB/04708/2020 with DOI 10.54499/UIDB/04708/2020 (https://doi.org/10.54499/UIDB/04708/2020) and Programmatic Funding -

UIDP/04708/2020 with DOI 10.54499/UIDP/04708/2020 (https://doi.org/10.54499/UIDP/04708/2020) of the CONSTRUCT - Instituto de I&D em Estruturas e Construções - funded by national funds through the FCT/MCTES (PIDDAC).

References

[1] A. Malekjafarian, P.J. McGetrick, E.J. Obrien, A review of indirect bridge monitoring using passing vehicles, Shock and Vibration 2015 (2015). https://doi.org/10.1155/2015/286139.

[2] Y.B. Yang, J.P. Yang, State-of-the-Art Review on Modal Identification and Damage Detection of Bridges by Moving Test Vehicles, International Journal of Structural Stability and Dynamics 18 (2018) 1850025. https://doi.org/10.1142/S0219455418500256.

[3] Y.B. Yang, C.W. Lin, J.D. Yau, Extracting bridge frequencies from the dynamic response of a passing vehicle, J Sound Vib 272 (2004) 471–493. https://doi.org/10.1016/S0022-460X(03)00378-X.

[4] C. Bragança, E.F. Souza, D. Ribeiro, A. Meixedo, T.N. Bittencourt, H. Carvalho, Drive-by Methodologies Applied to Railway Infrastructure Subsystems: A Literature Review—Part II: Track and Vehicle, Applied Sciences 13 (2023) 6982. https://doi.org/10.3390/app13126982.

[5] E.F. Souza, C. Bragança, A. Meixedo, D. Ribeiro, T.N. Bittencourt, H. Carvalho, Drive-by Methodologies Applied to Railway Infrastructure Subsystems: A Literature Review—Part I: Bridges and Viaducts, Applied Sciences 13 (2023) 6940. https://doi.org/10.3390/app13126940.

[6] The MathWorks Inc., MATLAB (R2020a), Natick, Massachusetts, 2020.

[7] UIC, Code 517 - Wagons - Suspension gear - Standardisation, (2007).

[8] C. Bragança, J. Neto, N. Pinto, P.A. Montenegro, D. Ribeiro, H. Carvalho, R. Calçada, Calibration and validation of a freight wagon dynamic model in operating conditions based on limited experimental data, Vehicle System Dynamics 60 (2022) 3024–3050. https://doi.org/10.1080/00423114.2021.1933091.

[9] ANSYS Inc., ANSYS® Academic Research Mechanical Release 18.1., (2018).

[10] J. Neto, P.A. Montenegro, C. Vale, R. Calçada, Evaluation of the train running safety under crosswinds - a numerical study on the influence of the wind speed and orientation considering the normative Chinese Hat Model, International Journal of Rail Transportation (2020) 1–28. https://doi.org/10.1080/23248378.2020.1780965.

[11] EN 13674-1, :2003+A1:2007 Railway applications. Track. Rail. Vignole railway rails 46 kg/m and above., (2006) 1–32.

[12] W. Zhai, K. Wang, C. Cai, Fundamentals of vehicle-track coupled dynamics, Vehicle System Dynamics 47 (2009) 1349–1376. https://doi.org/10.1080/00423110802621561.

[13] ERRI D 214, RP5 - Rail bridges for speeds> 200 km/h: Numerical investigation of the effect of track irregularities at bridge resonance, (1999).

[14] ERRI D 202, RP11 - Improved knowledge of forces in CWR track (including switches): Parametric study and sensitivity analysis of CWERRI Verification of an FEM for the buckling resistance of tracks with continuous welded rails (CWR), (1999).

[15] Y.S. Wu, Y. Bin Yang, Steady-state response and riding comfort of trains moving over a series of simply supported bridges, Eng Struct 25 (2003) 251–265. https://doi.org/10.1016/S0141-0296(02)00147-5.

[16] UIC, Code 774-3-R Track/Bridge interaction - Recomendations for calculation, (2001).

[17] J. Neto, P.A. Montenegro, C. Vale, R. Calçada, Evaluation of the train running safety under crosswinds - a numerical study on the influence of the wind speed and orientation considering the normative Chinese Hat Model, International Journal of Rail Transportation (2020) 1–28. https://doi.org/10.1080/23248378.2020.1780965.

[18] L. Bernardini, M. Carnevale, A. Collina, Damage identification in warren truss bridges by two different time–frequency algorithms, Applied Sciences (Switzerland) 11 (2021). https://doi.org/10.3390/app112210605.

[19] S.G.M. Neves, P.A. Montenegro, A.F.M. Azevedo, R. Calçada, A direct method for analyzing the nonlinear vehicle-structure interaction, Eng Struct 69 (2014) 83–89. https://doi.org/10.1016/j.engstruct.2014.02.027.

[20] P.A. Montenegro, S.G.M. Neves, R. Calçada, M. Tanabe, M. Sogabe, Wheel-rail contact formulation for analyzing the lateral train-structure dynamic interaction, Comput Struct 152 (2015) 200–214. https://doi.org/10.1016/j.compstruc.2015.01.004.

[21] H.R. Hertz, Ueber die Berührung fester elastischer Körper (On Contact Between Elastic Bodies), Journal Für Die Reine Und Angewandte Mathematik (Crelle's Journal) 1882 (1882). https://doi.org/10.1515/crll.1882.92.156.

[22] J.J. Kalker, The computation of three-dimensional rolling contact with dry friction, Int J Numer Methods Eng 14 (1979) 1293–1307. https://doi.org/10.1002/nme.1620140904.

[23] J.J. Kalker, Book of Tables for the Hertzian Creep-force Law, Faculty of Technical Mathematics and Informatics, Delft University of Technology, 1996. https://books.google.pt/books?id=Yrf5GgAACAAJ.